Environ Sci Pollut Res (2018) 25:672–682
https://doi.org/10.1007/s11356-017-0461-9

RESEARCH ARTICLE

Kinetics and pathways of Bezafibrate degradation in UV/chlorine process

Xue-Ting Shi[1] · **Yong-Ze Liu**[1] · **Yu-Qing Tang**[1] · **Li Feng**[1] · **Li-Qiu Zhang**[1]

Received: 8 August 2017 / Accepted: 9 October 2017 / Published online: 20 October 2017
© Springer-Verlag GmbH Germany 2017

Abstract UV/chlorine, as a novel disinfection method, has attracted great interest due to its effective removal for pathogenic microorganism and degradation of trace organic contaminants existed in water environment. This paper investigated the degradation kinetics and pathways of Bezafibrate (BZF), a typical antilipemic drug, during UV/chlorine process. The results showed that 92.3% of BZF was degraded after 20 min in UV/chlorine process. This indicated HO• and reactive chlorine species (RCSs) formed in UV/chlorine played the dominant role in degrading BZF. Observed rate constants of BZF degradation ($k_{obs,BZF}$) in UV/chlorine process increased linearly in a wide chlorine dosage from 0.1 to 1.0 mM, which implied that ClO• generated from the reactions of chlorine with HO• and Cl• could react with BZF rapidly. The steady-state kinetic modeling result proved this deduction and the rate constant of ClO• with BZF was fitted to be 5.0×10^8 M^{-1} s^{-1}. $k_{obs,BZF}$ was affected by Cl^- and HA. The total contribution of RCSs (including Cl•, Cl_2•$^-$, and ClO•) to the degradation of BZF was determined to be ~ 80%, which is much higher than that of HO•. Thirteen degradation products of BZF were identified by LC-MS/MS. Initial degradation products were arisen from hydroxylation, chlorine substitution and cyclization by HO• and RCSs, and then further oxidized to generate acylamino cleavage and demethylation products.

Keywords UV/chlorine process · Bezafibrate · Degradation kinetics and pathways · Reactive chlorine species

Responsible editor: Bingcai Pan

Electronic supplementary material The online version of this article (https://doi.org/10.1007/s11356-017-0461-9) contains supplementary material, which is available to authorized users.

✉ Li-Qiu Zhang
zhangliqiu@163.com

[1] Beijing Key Lab for Source Control Technology of Water Pollution, College of Environmental Science and Engineering, Beijing Forestry University, No. 35 Tsinghua East Road, Beijing 100083, People's Republic of China

Introduction

The widespread occurrence of pharmaceutical and personal care products (PPCPs) in aquatic environments has received great attention in recent years (Mompelat et al. 2009). PPCPs are frequently detected in treated sewage, surface and ground water at concentrations of nanogram per liter to microgram per liter (Cai et al. 2013; Kim et al. 2007; Kosma et al. 2010). Traditional water treatment processes cannot effectively remove PPCPs which makes PPCPs widely exist in public and threaten public health and ecological environment (Beretta et al. 2014; Mitch and Sedlak 2004; Watkinson et al. 2009; Zhao et al. 2014). Disinfection process, one of the essential drinking water and wastewater treatment technologies, acts a significant role not only in terms of inactivating pathogenic microorganisms but also in removing trace PPCPs (Kosma et al. 2010; Simazaki et al. 2008). Chlorination and UV irradiation were the most frequently used disinfection methods by far all over the world (Gibs et al. 2007; Glassmeyer and Shoemaker 2005; Kim and Tanaka 2009; Lee and von Gunten 2010). Although chlorine can degrade some PPCPs containing electron-donating moieties efficiently such as phenol and aniline groups (Lee et al. 2007), they cannot degrade some refractory PPCPs successfully such as phenytoin and atenolol (Huerta-Fontela et al. 2011). Besides, indomethacin and metoprolol are poorly degraded by UV irradiation at conventional disinfection dose rates (up to 5.0×10^2 mJ cm^{-2}) (Kim et al. 2009). Therefore, combining UV irradiation and

chlorine (UV/chlorine) has attracted great interest in recent years (Yang et al. 2016).

It has been reported that UV/chlorine process can degrade many PPCPs effectively containing trichloroethylene, chlortoluron, ibuprofen, carbamazepine, and diclofenac (Guo et al. 2016). It is known that hydroxyl radical (HO•) and reactive chlorine radicals such as Cl• can be produced in UV/chlorine process (as shown in Eq. (1)) (Fang et al. 2014). HO• is non-selective and could react with various contaminants at almost diffusion-controlled rates, whereas Cl• is a selective oxidant that is more likely to react with compounds containing aromatic ring and electron rich moieties (Buxton et al. 1988; Mártire et al. 2001). Moreover, Cl• reacts with chloride to produce $Cl_2^{\bullet-}$ (Eq. (6)), and both HO• and Cl• react with HClO/ClO^- to produce ClO• (Eqs. (2)~(5)). $Cl_2^{\bullet-}$ and ClO• also react selectively with contaminants (Buxton et al. 1988). The coexisting substances including carbonate, chloride ion, and humic acid (HA), which are normally present in water, may consume chlorine or as radical scavenger and thereby affect the removal of PPCPs (Yang et al. 2016). The variety of radical species including HO• and reactive chlorine species (RCSs, i.e., Cl•, $Cl_2^{\bullet-}$, ClO•) may make UV/chlorine process a complex system for the degradation of PPCPs.

$$HOCl/OCl^- + h\nu \rightarrow HO\bullet + Cl\bullet \quad (1)$$

$$HO\bullet + HClO \rightarrow H_2O + ClO\bullet \quad k = 8.46 \times 10^4 M^{-1}s^{-1} \quad (2)$$

$$ClO^- + HO\bullet \rightarrow OH^- + ClO\bullet \quad k = 8.8 \times 10^9 M^{-1}s^{-1} \quad (3)$$

$$Cl\bullet + HClO \rightarrow H^+ + Cl^- + ClO\bullet \quad k = 3.0 \times 10^9 M^{-1}s^{-1} \quad (4)$$

$$Cl\bullet + OCl^- \rightarrow Cl^- + ClO\bullet \quad k = 8.2 \times 10^9 M^{-1}s^{-1} \quad (5)$$

$$Cl^- + Cl\bullet \leftrightarrow Cl_2^{\bullet-} \quad k_+ = 6.5 \times 10^9 M^{-1}s^{-1}; k_- = 1.1 \times 10^5 s^{-1} \quad (6)$$

Bezafibrate (BZF) is a typical antilipemic drug with an estimated annual consumption of several hundreds of tons in developed countries (Yuan et al. 2012). In Germany, BZF has been found in the effluents of wastewater treatment plants (WWTPs) with concentrations up to 4.6 μg L^{-1} and median value of 2.2 μg L^{-1} (Szabó 2010; Trovó et al. 2008). In surface waters, BZF has been identified at median concentration of 3.1 μg L^{-1} (Gonçalves et al. 2013). BZF is refractory to biological treatment process (Razavi et al. 2009). The chronic effects and ecological risk potential of BZF in surface water and WWTPs make the viability of the reclamation of wastewater disputable (Cermola et al. 2005; Dantas et al. 2007; Trovó et al. 2008; Yuan et al. 2012). The abatement of BZF from water has been investigated using different advanced oxidation processes (AOPs) (Lambropoulou et al. 2008; Xu et al. 2016; Yuan et al. 2012). However, the use of UV/chlorine as AOP for BZF removal, and the kinetics and mechanisms of this process, have not been reported.

The present study primarily investigated the kinetics of BZF degradation during UV/chlorine process, and further examined the effects of chlorine concentration, BZF concentration, pH, HCO_3^-, Cl^-, humic acid (HA) on the degradation of BZF. In addition, the contributions of each reactive species (i.e., HO• and RCSs) in UV/chlorine process to BZF degradation were illuminated. Finally, the degradation intermediates and by-products were monitored to reveal BZF degradation pathway in UV/chlorine process.

Materials and methods

Chemicals and materials

BZF (purity > 98%) and sodium hypochlorite (NaClO) including 13% available free chlorine were obtained from Sigma-Aldrich. Other chemicals including nitrobenzene (NB, purity > 99%), H_2O_2 solution (35%, *w*/*w*), potassium peroxodisulfate ($S_2O_8^{2-}$), and acetic acid were obtained from Aladdin (China). Methanol and acetonitrile (J.T. Baker Inc., USA) were HPLC grade. All of other reagents were purchased as analytical grade or higher and were used without further purification, such as NaOH (99% AR), phosphate (95% AR), and HA (AR). All solutions were prepared with ultrapure water (UPW) from a Water Purification System (Cascada TM LS). HA was dissolved in NaOH solution and then filtered by 0.45-μm glass fiber membrane.

Experimental instrument

The experimental UV device was produced by a straight beam of 254 nm low-pressure UV mercury lamp (GPH212T5L/4, 10 W, Heraeus). A reactor (height of 4 cm) containing reaction solution of 100 mL was placed under the UV device of the collimator tube. As shown in Fig. S1 in supporting information, the UV lamps were set at about 30 cm above a glass reactor with a quartz cap. The photon lux (I_0, 253.7 nm) of UV irradiation of solution was determined to be 1.291×10^{-7} Einstein L^{-1} s^{-1} by iodine iodide chemical actinometry (Rahn et al. 2003) and light intensity at surface of solution was detected by irradiatometer to be 0.16 mW cm^{-2}. A stirring in appropriate size was placed in reactor to ensure homogeneous ultraviolet irradiation. All experiments were conducted at room temperature (20 ± 1 °C).

Kinetic experiments of BZF degradation in pure water

The reactor is an amber borosilicate bottle (110 mL). All experiments were carried out in pseudo-first-order conditions ($[chlorine]_0/[BZF]_0 > 10$) in homogeneous solution. The kinetic experiments were performed by placing specific concentration of NaClO and BZF solution on the experimental UV device (Fig. S1 in the supporting information). The reaction volume was controlled at 100 mL. One-milliliter sample was

taken from the reactor at a fixed time interval and immediately quenched with 0.01 ml of ascorbic acid (0.1 M) (Lyon et al. 2014). Previous tests proved that ascorbic acid did not affect the detection of BZF. All samples were filtrated by a 0.22-μM glass fiber membrane and were further analyzed by high performance liquid chromatography (HPLC) to obtain the residual concentration of BZF. All experiments were repeated at least twice.

The buffer solution of 10 mM phosphate (KH_2PO_4) was used for adjusting the solution pH. The effect of phosphate on BZF degradation was confirmed to be very slight and could be ignored (Fig. S2 in supporting information).

The experiments of BZF degradation in UV irradiation and in chlorination alone were also followed the above procedures while only NaClO or UV photolysis spiked into the reactor. In addition, the degradation of BZF in UV/H_2O_2 and UV/$S_2O_8^{2-}$ systems was also carried out in the same manner using H_2O_2 and $K_2S_2O_8$ to substitute NaClO.

Effects of different factors on BZF degradation in UV/chlorine process

To investigate the effects of chlorine dosage, BZF concentration, and real water matrixes on BZF degradation, the following experiments were carried out.

Real water matrixes including HCO_3^-, Cl^-, and HA are normally exist in surface water and wastewater, and act dominated roles in the production of radical species (Kong et al. 2016; Wang et al. 2016). Experiments under different chlorine, BZF, HCO_3^-, Cl^-, and HA concentration were conducted following the above manners to investigate the effect of different factors on BZF degradation rate.

Contributions of HO• and RCSs to BZF degradation

Experiments under different pH (5.0, 6.0, 7.0, and 8.0) were conducted at 0.8 mM chlorine concentration and 10 μM BZF concentration to study the impact of pH on BZF reaction rates.

The steady-state concentrations of HO• ($[HO•]_{ss}$) at different pH (5.0, 6.0, 7.0 and 8.0) in UV/chlorine process could be obtained using nitrobenzene (NB) as the HO• probe compound. NB reacts with HO• with high second-order rate constant of $k_{HO•-NB} = 3.9 \times 10^9\ M^{-1}\ s^{-1}$ and its reaction with RCSs could be ignored (Watts and Linden 2007). The rates of BZF degradation by RCSs ($k_{obs,RCSs-BZF}$) could be calculated as Eqs. (7) and (8).

$$k_{HO•-NB}[HO•]_{ss} = k_{obs,NB} \quad (7)$$

$$k_{HO•-BZF}[HO•]_{ss} + k_{obs,RCSs-BZF} = k_{obs,BZF} \quad (8)$$

The second-order rate constants of reaction of BZF with HO• ($k_{HO•-BZF}$) is $8.0 \times 10^9\ M^{-1}\ s^{-1}$. The observed rate constant of NB ($k_{obs,NB}$) and BZF ($k_{obs,BZF}$) were obtained by experiments and $[HO•]_{ss}$ could be calculated by Eq. (7). Then, $k_{obs,RCSs-BZF}$ could be obtained by $k_{obs,BZF}$ deducting the $k_{HO•-BZF}[HO•]_{ss}$.

Experiment was conducted with coexistence of BZF (10 μM) and NB (10 μM). The concentration of chlorine was controlled at 0.8 mM and the solution pH was adjusted to 5.0, 6.0, 7.0, and 8.0. Other manner was similar to "Kinetic experiments of BZF degradation in pure water" section described above.

Identification of BZF degradation products

In the experiment of determining BZF degradation intermediates during UV/chlorine process, the relatively high concentrations of 0.5 mM BZF and 1.6 mM chlorine were applied in order to acquire more complete and accurate degradation intermediates. At the scheduled time (10, 25, 40, 60, 90, 130, 190, 250 min), 1 mL sample was withdrawn, quenched with ascorbic acid which did not interfere the detection of BZF and its intermediates.

Analytical methods

Analysis of free chlorine concentrations

The concentrations of free chlorine in the reactor were obtained by the *N*,*N*-diethyl-p-phenylenediamine (DPD) method (Carranzo 2012). DPD with free chlorine could result to chromogenic reaction and the resulting compound can absorb ultraviolet light at 515 nm. Concentration of free chlorine was calculated by measured absorbance.

Analysis of BZF and NB concentration

Concentrations of BZF and NB were analyzed through HPLC system (Agilient 1260 series, USA) by a Poroshell 120 EC-C18 column (4.6 mm × 50 mm 2.7 μm, Agilent, USA) and the UV detector was set at 227 and 262 nm, respectively. The flow rate of the column was 1.0 mL/min with the temperature maintained at 30 °C. The composition of the mobile phase for the analysis of BZF and NB was 55% acetic acid (0.02 vol.%, pH = 4), 5% methanol, 40% acetonitrile, 50% water, and 50% methanol, respectively.

Analysis of BZF degradation products

The degradation intermediates of BZF were measured by liquid chromatography-tandem mass spectrometry (LC-MS/MS, Thermo Scientific QExactive plus). The sample (0.2 mL min^{-1}) was delivered by a gradient system from a Waters BEH C18 (1.7 μM × 100 mm) column. The consist of mobile phase was acetonitrile solution (A) and 0.1% formic acid (B), which was eluted according to the following gradient

mode: (1) 90% B from 0 to 1 min; (2) from 1 to 15 min, A was increased in a linearly fashion from 10 to 50%; (3) from 15 to 22 min, A was increased in a linearly fashion from 50 to 99% and set for 3 min; and (4) the mobile phase was returned to its initial composition from 25 to 30 min.

Kinetic modeling

To get insight into the role of the reactive radicals to BZF degradation in UV/chlorine process, a kinetic model considering different radical species was established. The Matlab model was established based on the observation that BZF was mainly degraded by the reactive radicals in the UV/chlorine process such as HO•, ClO•, $Cl_2^{\bullet-}$, and Cl•. The contributions of other radicals such as $ClOH^{\bullet-}$ and $O^{\bullet-}$ in the process had a negligible effect owing to their low reactivity with organic compounds (Guo et al. 2016). Table S1 in supporting information lists the principal reactions and their rate constants in UV/chlorine from the literatures.

The BZF degradation followed pseudo-first-order kinetic in the UV/chlorine process, thus can be modeled as follows:

$$d[\mathrm{BZF}]/dt = \left(k_{30}[\mathrm{HO}\bullet]_{ss} + k_{31}[\mathrm{Cl}\bullet]_{ss} + k_{32}[\mathrm{Cl_2}^{\bullet-}]_{ss} + k_{33}[\mathrm{ClO}\bullet]_{ss}\right)[\mathrm{BZF}] = k_{\mathrm{obs,BZF}}[\mathrm{BZF}] \quad (9)$$

where $[HO\bullet]_{ss}$, $[Cl\bullet]_{ss}$, $[Cl_2^{\bullet-}]_{ss}$, and $[O^{\bullet-}]_{ss}$ are the steady-state concentrations of HO•, Cl•, $Cl_2^{\bullet-}$, and $O^{\bullet-}$; $k_{obs,BZF}$ is the overall pseudo-first-order rate constant of BZF degradation. Based on these principal reactions (Table S1 in supporting information), the kinetic expressions of HO•, Cl•, $Cl_2^{\bullet-}$, $O^{\bullet-}$, $ClOH^{\bullet-}$, and ClO• in UV/chlorine process are shown in Eqs. (10)–(15), where $r_{HO\bullet}$, $r_{O\bullet-}$, and $r_{Cl\bullet}$ in Eqs. (10), (13), and (11) are the formation rates of HO•, $O^{\bullet-}$, and Cl• from the photolysis of chlorine (shown in Table S1 in supporting information).

$$d[\mathrm{HO}\bullet]/dt = r_{\mathrm{HO}\bullet} + k_{19}[\mathrm{ClOH}^{\bullet-}] + k_{17}[\mathrm{O}^{\bullet-}][\mathrm{H_2O}] - k_{30}[\mathrm{HO}\bullet][\mathrm{BZF}] - k_{13}[\mathrm{HO}\bullet][\mathrm{HClO}] - k_{14}[\mathrm{HO}\bullet][\mathrm{ClO}^-] - k_{39}[\mathrm{HO}\bullet][\mathrm{Cl}^-] - k_{12}[\mathrm{HO}\bullet][\mathrm{HO}^-] \quad (10)$$

$$d[\mathrm{Cl}\bullet]/dt = r_{\mathrm{Cl}\bullet} + k_{42}[\mathrm{Cl_2}^{\bullet-}] + k_{20}[\mathrm{ClOH}^{\bullet-}] + k_{21}[\mathrm{ClOH}^{\bullet-}][\mathrm{H}^+] - k_{31}[\mathrm{Cl}\bullet][\mathrm{BZF}] - k_{42}[\mathrm{Cl}\bullet][\mathrm{Cl}^-] - k_9[\mathrm{Cl}\bullet][\mathrm{HClO}] - k_{10}[\mathrm{Cl}\bullet][\mathrm{ClO}^-] - k_8[\mathrm{Cl}\bullet][\mathrm{HO}^-] \quad (11)$$

$$d[\mathrm{Cl_2}^{\bullet-}]/dt = k_{42+}[\mathrm{Cl}\bullet][\mathrm{Cl}^-] + k_{22}[\mathrm{Cl}^-][ClOH^{\bullet-}] - k_{42-}[\mathrm{Cl_2}^{\bullet-}] - k_{32}[\mathrm{Cl_2}^{\bullet-}][\mathrm{BZF}] - k_{14}[\mathrm{Cl_2}^{\bullet-}][\mathrm{HO}^-] \quad (12)$$

$$d[\mathrm{O}^{\bullet-}]/dt = r_{\mathrm{O}^{\bullet-}} + k_{12}[\mathrm{HO}\bullet][\mathrm{HO}^-] - k_{17}[\mathrm{O}^{\bullet-}][\mathrm{H_2O}] \quad (13)$$

$$d[ClOH^{\bullet-}]/dt = k_3[\mathrm{HO}\bullet][\mathrm{Cl}^-] + k_8[\mathrm{Cl}\bullet][\mathrm{HO}^-] + k_{25}[\mathrm{Cl_2}^{\bullet-}][\mathrm{HO}^-] - k_{19}[ClOH^{\bullet-}] - k_{21}[ClOH^{\bullet-}][\mathrm{H}^+] - k_{22}[ClOH^{\bullet-}][\mathrm{Cl}^-] \quad (14)$$

$$d[\mathrm{ClO}\bullet]/dt = k_{13}[\mathrm{HO}\bullet][\mathrm{ClO}^-] + k_9[\mathrm{Cl}\bullet][HClO] + k_{14}[\mathrm{HO}\bullet][\mathrm{ClO}^-] + k_{10}[\mathrm{HO}\bullet][HClO] - k_{27}[\mathrm{ClO}\bullet][\mathrm{ClO}\bullet] - k_{25}[\mathrm{ClO}\bullet][\mathrm{BZF}] \quad (15)$$

Under the steady-state conditions, the formation rates of radicals are equal to their consumption rates. Therefore, the net formation rates of HO•, Cl•, $Cl_2^{\bullet-}$, $O^{\bullet-}$, $ClOH^{\bullet-}$, and ClO• are approximately zero. Some concerned parameters such as the initial concentrations of Cl^-, H^+, HO^-, HClO, and ClO^- were input in the model (for details, see Text S1 in supporting information), and thus the steady-state concentrations of HO•, Cl•, $Cl_2^{\bullet-}$, $O^{\bullet-}$, $ClOH^{\bullet-}$, and ClO• could be calculated from Matlab. Knowing the rate constants and steady-state concentrations of HO•, Cl•, $Cl_2^{\bullet-}$, $O^{\bullet-}$, $ClOH^{\bullet-}$, and ClO•, the $k_{obs,BZF}$ values of the BZF degradation and the specific contributions of various radicals under different chlorine dosage could be calculated according to Eq. (9).

Results and discussion

Kinetics of BZF degradation in pure water

Figure 1 shows the time-depended of BZF concentrations in UV/chlorine process, taking UV irradiation, dark chlorination, UV/H_2O_2 and UV/$S_2O_8^{2-}$ processes as comparison. It can be seen that 92.3% of BZF was degraded after 20 min in UV/chlorine process, while only 1.2 and 4.0% of BZF were degraded in UV irradiation and in chlorination alone,

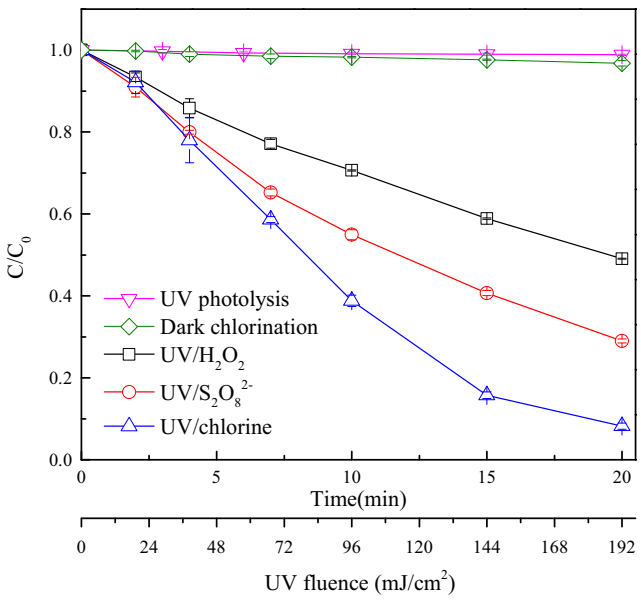

Fig. 1 BZF degradation in UV/chlorine, UV irradiation, dark chlorination, UV/H_2O_2, and UV/$S_2O_8^{2-}$ processes. Experimental conditions: I_0 = 1.291 × 10^{-7} Einstein L^{-1} s^{-1}, [NaClO] = 0.8 mM, [BZF] = 10 μM, pH = 7.0, 10 mM phosphate buffer, T = 20 ± 1 °C

indicating the recalcitrance of BZF to UV irradiation and chlorination alone. The degradation of BZF in UV/chlorine, UV/H_2O_2, and UV/$S_2O_8^{2-}$ processes followed the pseudo-first-order kinetics (as shown in Fig. 2 and Fig. S3 in supporting information), and the rate constants were obtained to be 1.98×10^{-3}, 5.87×10^{-4}, and 1.03×10^{-3} s^{-1}, respectively. The rate constant of UV/chlorine is 3.4 times and 1.9 times higher than that of UV/H_2O_2 and UV/$S_2O_8^{2-}$ systems which could be explained that chlorine has higher radical production than H_2O_2 and $S_2O_8^{2-}$. The rate of radical production can be obtained by Table S1 in supporting information, which was greatly affected by the quantum yields and the molar absorption coefficients (λ = 254 nm) of oxidants. The quantum yields of HClO, ClO^-, H_2O_2, and $S_2O_8^{2-}$ in UV irradiation are 1.45, 0.7, 0.5, and 0.7, respectively, and the molar absorption coefficients of HClO, ClO^-, H_2O_2, and $S_2O_8^{2-}$ are 59, 66, 19.6, and 21.1 M^{-1} cm^{-1}, respectively (Guan et al. 2011; Hessler et al. 2010; Z et al. 2014). Obviously, HClO and ClO^- have larger quantum yield and molar absorption coefficients than H_2O_2 and $S_2O_8^{2-}$.

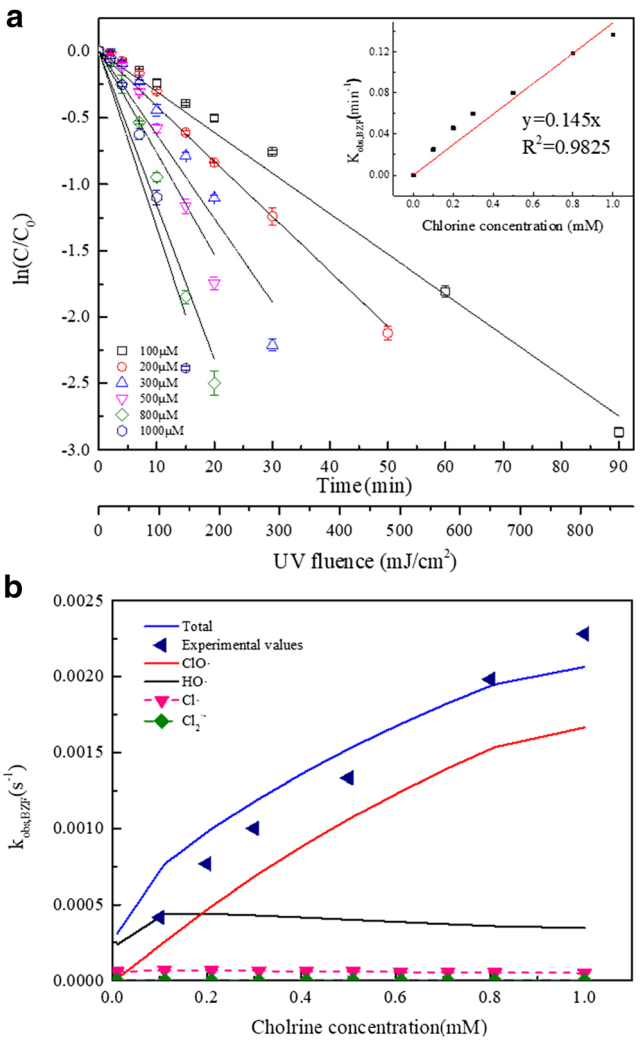

Fig. 2 BZF degradation in UV/chlorine process at different initial chlorine concentrations. Experimental conditions: $I_0 = 1.291 \times 10^{-7}$ Einstein L^{-1} s^{-1}, [NaClO] = 0.1 ~ 1.0 mM, [BZF] = 10 μM, pH = 7.0, 10 mM phosphate buffer, $T = 20 \pm 1$ °C

Effects of different factors on BZF degradation in UV/chlorine process

Effect of chlorine concentration on BZF degradation

Figure 2 showed that the BZF degradation rate increased with the increase of chlorine dosage. The observed BZF degradation followed pseudo-first-order reactions, and thus the rate can be given as Eq. (16) as follows:

$$\ln\left([BZF]/[BZF]_0\right) = -k_{obs,BZF} \times t \quad (16)$$

where [BZF] and $[BZF]_0$ stand for the concentrations of BZF at time t and 0, respectively. Therefore, the observed rate constant of BZF degradation, $k_{obs,BZF}$, can be obtained by linear fitting of data of natural logarithm of normalized concentration of BZF versus time (Fig. 2a).

As shown in Fig. 2a (Insert), $k_{obs,BZF}$ increased linearly from 5.1×10^{-4} to 2.24×10^{-3} s^{-1} with the increase of initial chlorine concentration in the wide range from 0.1 to 1.0 mM. Previous studies have observed plateaus of k_{obs} for benzoic acid (BA) and atrazine (ATZ) with the increase of chlorine (0.01 ~ 0.12 and 0.02 ~ 0.1 mM) (Fang et al. 2014; Kong et al. 2016). However, this plateau was not observed at the case of BZF in the present study. To get insight into the roles of reactive radicals on BZF degradation at different chlorine concentrations, a Matlab model was established consisting of the principal reaction in UV/chlorine process (as described in "Kinetic modeling"section). According to the calculation of

Table 1 The steady-state concentrations of different reactive radicals in UV/chlorine process at different chlorine dosage

Chlorine dosage (mM)	HO• concentration (M)	Cl• concentration (M)	ClO• concentration (M)
0.01	1.32×10^{-13}	1.18×10^{-13}	2.71×10^{-14}
0.10	2.44×10^{-13}	1.38×10^{-13}	5.14×10^{-13}
0.20	2.45×10^{-13}	1.33×10^{-13}	9.79×10^{-13}
0.30	2.38×10^{-13}	1.28×10^{-13}	1.41×10^{-12}
0.40	2.31×10^{-13}	1.23×10^{-13}	1.80×10^{-12}
0.50	2.23×10^{-13}	1.18×10^{-13}	2.16×10^{-12}
0.60	2.15×10^{-13}	1.14×10^{-13}	2.49×10^{-12}
0.70	2.07×10^{-13}	1.10×10^{-13}	2.79×10^{-12}
0.80	2.00×10^{-13}	1.06×10^{-13}	3.07×10^{-12}
0.90	1.93×10^{-13}	1.02×10^{-13}	3.33×10^{-12}
1.0	1.90×10^{-13}	1.01×10^{-13}	3.70×10^{-12}

model, the steady-state concentrations of different reactive radicals at different chlorine concentrations were obtained. As shown in Table 1, with the increase of chlorine concentrations, the steady-state concentrations of HO• and Cl• increased from 1.32×10^{-13} and 1.18×10^{-13} M to 2.44×10^{-13} and 1.38×10^{-13} M at low chlorine dosage (0.01 ~ 0.1 mM), and reached plateaus at high chlorine dosage (0.1 ~ 1.0 mM). The appearance of this plateau was ascribed to the scavenging of HO• and Cl• by excessive HClO/ClO^- at high chlorine dosage (0.1 ~ 1.0 mM), resulting in the counterbalance between the formation and the consumption of HO• and Cl•, as shown in Eqs. (1)~(5). The plateaus of steady-state concentrations of HO• and Cl• could well explain the previous observed plateaus of k_{obs} for BA and ATZ (Fang et al. 2014; Kong et al. 2016), while fail to elaborate the continuously linear increase of k_{obs} for BZF with the increase of chlorine dosage. It should be noted that the concentration of ClO• continually increased with the increase of chlorine dosage, which was different from HO• and Cl•, as shown in Table 1. This is reasonable because HClO/ClO^- did not scavenge ClO• yet. It seems likely that the reactive radical ClO• in UV/chlorine process could also oxidize BZF with a appreciate rate constant. However, the second-order rate constant of BZF with ClO• was not available in the literature, and was fitted to be 5.0×10^8 M^{-1} s^{-1} by the consistence of the simulated result with the experimental data, as shown in Fig. 2b. This conclusion was consistent with the previous speculation which explained similar linear increase of k_{obs} for trimethoprim (THM) in UV/chlorine process with the increase of the chlorine dosage (Wu et al. 2016).

Effects of BZF concentration on BZF degradation

Figure 3 shows the degradation of BZF at different initial BZF concentrations (5.0 ~ 25 μM). It can be found the $k_{obs,BZF}$ decreased as the initial BZF concentration increased from 5.0 to 25 μM. The molar absorptivity of BZF at 254 nm is $(1.40 \pm 0.24) \times 10^4$ M^{-1} cm^{-1} (Wols et al. 2015), which was much higher than that of HClO (59 M^{-1} cm^{-1}) and ClO^- (66 M^{-1} cm^{-1}). With the increase of BZF concentration, BZF might compete more photon than HClO and ClO^-, and reduce the production rates of HO• and RCSs, and then decreased the degradation of BZF.

Effects of HCO_3^-, Cl^-, and HA on BZF degradation

As shown in Fig. 4, the concentration of 0 ~ 40 mM HCO_3^- showed negligible effect on BZF degradation in UV/chlorine process. The HCO_3^- may compete BZF for HO• and Cl• consumption. For example, at higher HCO_3^- concentration of 40 mM in this experiment, the rate constants for the reactions of HCO_3^- with HO• and Cl• were 3.4×10^5 s^{-1} (i.e., 8.5×10^6 M^{-1} s^{-1} × 40 mM = 3.4×10^5 s^{-1}) and 8.8×10^6 s^{-1} ($k_{obs} = 2.2 \times 10^8$ M^{-1} s^{-1} × 40 mM = 8.8×10^6 s^{-1}), respectively. These were much higher than the rate constants for the reactions of BZF with HO• and Cl•, which were 8.0×10^4 s^{-1} (i.e., 8.0×10^9 M^{-1} s^{-1} × 10 μM = 8.0×10^4 s^{-1}) and 5.0×10^3 s^{-1} (i.e., 5.0×10^8 M^{-1} s^{-1} × 10 μM = 5.0×10^3 s^{-1}), respectively. HCO_3^- scavenges HO• and Cl• to form $CO_3^{\bullet-}$ (Eqs. (17)~(19)).

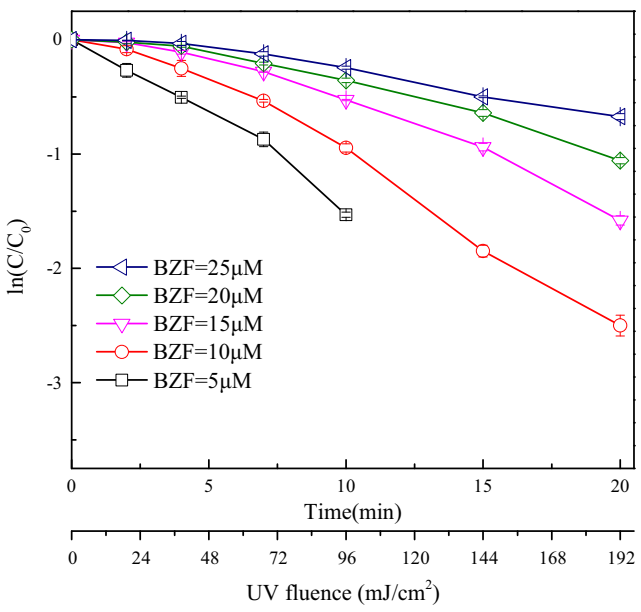

Fig. 3 BZF degradation in UV/chlorine process at different initial BZF concentrations. Experimental conditions: $I_0 = 1.291 \times 10^{-7}$ Einstein L^{-1} s^{-1}, [NaClO] = 0.8 mM, [BZF] = 5.0 ~ 25 μM, pH = 7.0, 10 mM phosphate buffer, $T = 20 \pm 1$ °C

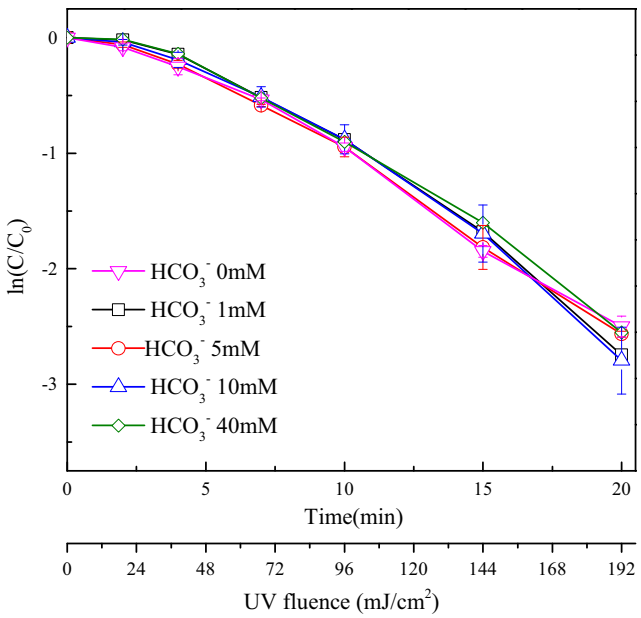

Fig. 4 BZF degradation in UV/chlorine process in the presence of different HCO_3^- concentrations. Experimental conditions: $I_0 = 1.291 \times 10^{-7}$ Einstein L^{-1} s^{-1}, [NaClO] = 0.8 mM, [BZF] = 10 μM, [$NaHCO_3$] = 0 ~ 40 mM, pH = 7.0, 10 mM phosphate buffer, $T = 20 \pm 1$ °C

No inhibition effect on BZF degradation was observed experimentally suggesting that CO_3•$^-$ was likely to react with BZF. It has been reported $CO_3^{\bullet-}$ could react quickly with the uracil functional group in amine at rate constants of $1.4 \times 10^8 \sim 9.1 \times 10^8$ M^{-1} s^{-1} (Zhang et al. 2015). Therefore, the rate constant of BZF with $CO_3^{\bullet-}$ was presumed to be in the magnitude of $10^8 \sim 10^9$ M^{-1} s^{-1}, which is comparable with HO• (8.0×10^9 M^{-1} s^{-1}) and Cl• (5.0×10^8 M^{-1} s^{-1}).

$$HCO_3^- + HO\bullet \rightarrow H_2O + CO_3^{\bullet-} \quad k = 8.5 \times 10^6 M^{-1}s^{-1} \quad (17)$$

$$HCO_3^- + Cl\bullet \rightarrow H^+ + Cl^- + CO_3^{\bullet-} k = 2.2 \times 10^8 M^{-1}s^{-1} \quad (18)$$

$$ClO\bullet + CO_3^{2-} \rightarrow ClO^- + CO_3^{\bullet-} k = 6.0 \times 10^2 M^{-1}s^{-1} \quad (19)$$

The BZF degradation in the presence of Cl^- (0 ~ 100 mM) was shown in Fig. 5. It can be seen that the effect of the presence of low concentration of Cl^- (0 ~ 10 mM) on BZF degradation could be neglected, while high concentration of Cl^- (10 ~ 100 mM) slightly improved the removal efficiency of BZF. Generally, $Cl_2^{\bullet-}$ and Cl• can be formed by Cl^- reacting with Cl• and HO• in acid solution, which are more selective than HO• (Eqs. (20)~(22)). In neutral solution (pH = 7.0), at low concentration of Cl^- (0 ~ 10 mM), the rate constant of reverse reaction of Eq. (20) (6.1×10^9 s^{-1}) is much higher than Eq. (21) (2.1×10^3 s^{-1}), thereby making $ClOH^{\bullet-}$ preferring to turn to HO•, rather than Cl•, which caused neglected effect on BZF degradation. However, higher concentration of Cl^- (10 ~ 100 mM) in neutral solution could accelerate the reaction Eq. (20) and generate more $ClOH^{\bullet-}$, thereby promoting the production of Cl• and $Cl_2^{\bullet-}$ and then influencing the BZF degradation. The promoted effect suggested that BZF might react with $Cl_2^{\bullet-}$ with high rate constant. Similarly, a previous study found that the existence of Cl^- enhanced 4-tert-butylphenol (4tBP) degradation in Fe(III)-EDDS/$S_2O_8^{2-}$/UV process significantly, and the high reactivity of $Cl_2^{\bullet-}$ with 4tBP was proposed(Wu et al. 2015).

$$HO\bullet + Cl^- \leftrightarrow ClOH^{\bullet-} \quad k_+ = 4.3 \times 10^9 M^{-1}s^{-1}; k_- = 6.1 \times 10^9 s^{-1} \quad (20)$$

$$ClOH^{\bullet-} + H^+ \leftrightarrow Cl\bullet + H_2O k_+ = 2.1 \times 10^{10} M^{-1}s^{-1}; k_- = 2.5 \times 10^5 M^{-1}s^{-1} \quad (21)$$

$$Cl^- + Cl\bullet \leftrightarrow Cl_2^{\bullet-} k_+ = 6.5 \times 10^9 M^{-1}s^{-1}; k_- = 1.1 \times 10^5 M^{-1}s^{-1} \quad (22)$$

The influence of HA concentration on BZF degradation in UV/chlorine process was shown in Fig. 6 and the results showed obvious inhibited effect on BZF degradation. HA may compete with BZF for HO• and Cl• consumption as a radical scavenger, and also absorbs UV light at 254 nm with extinction coefficient of 3.15 L m^{-1} mg^{-1} so it is an inner filter to reduce the efficiency of chlorine photolysis in producing radicals (e.g., HO• and Cl•) (Wu et al. 2016).

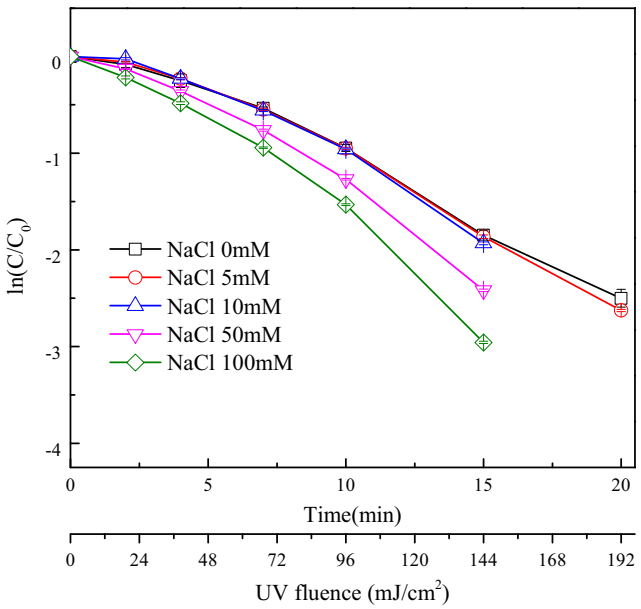

Fig. 5 BZF degradation in UV/chlorine process at the presence of different Cl^- concentrations. Experimental conditions: $I_0 = 1.291 \times 10^{-7}$ Einstein L^{-1} s^{-1}, [NaClO] = 0.8 mM, [BZF] = 10 μM, [NaCl] = 0 ~ 100 mM, pH = 7.0, 10 mM phosphate buffer, $T = 20 \pm 1$ °C

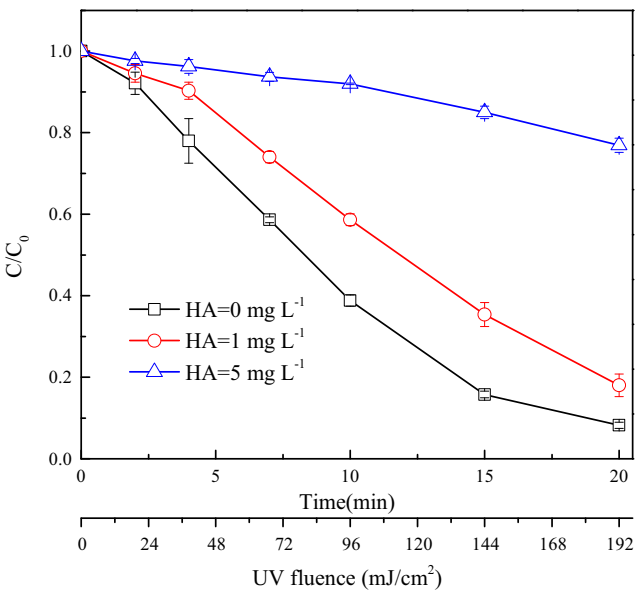

Fig. 6 BZF degradation in UV/chlorine process at the presence of different HA concentrations. Experimental conditions: $I_0 = 1.291 \times 10^{-7}$ Einstein L^{-1} s^{-1}, [NaClO] = 0.8 mM, [BZF] = 10 μM, [HA] = 0 ~ 5.0 mg L^{-1}, pH = 7.0, 10 mM phosphate buffer, $T = 20 \pm 1$ °C

Contributions of radical species to BZF degradation in UV/chlorine process

BZF was degraded rapidly during UV/chlorine process while it was hardly degraded in UV irradiation and chlorination alone (Fig. 1). This suggested that BZF was mainly degraded by the essential radical reactions in UV/chorine process. The HO• and RCSs (Cl•, $Cl_2^{\bullet-}$, and ClO•) are the main radical species from Eqs. (1)~(5) in UV/chlorine process. The contributions of HO• and RCSs to BZF degradation in UV/chlorine process at pH 5.0 ~ 8.0 were evaluated by addition of NB as a HO• probe compound (as described in "Contributions of HO• and RCSs to BZF degradation" section).

Figure 7 shows the calculated $k_{obs,BZF}$ by HO• and RCSs oxidation in UV/chlorine process at pH 5 ~ 8. The $k_{obs,BZF}$ decreased as pH increased from 5.0 to 8.0, and similar results were found in previous studies in which ibuprofen and trichloroethylene were taken as target compounds (Fang et al. 2014; Wang et al. 2012). This result could be explained by that at acidic pH, the dominant species of free chlorine is HClO, which has higher quantum yield and smaller radical scavenging effect than ClO^- shown in Table S1 in supporting information (Fang et al. 2014).

At pH 5.0, the contributions of HO• and RCSs to BZF degradation were about 36 and 64%, respectively. The contribution of HO• to BZF degradation decreased to about 20%, whereas the contribution of RCSs increased to about 80% with increasing pH from 5.0 to 8.0. Similar results were observed in ibuprofen degradation in UV/chlorine process, where the RCSs contributed more in alkaline solutions than in acidic solutions (Xiang et al. 2016).

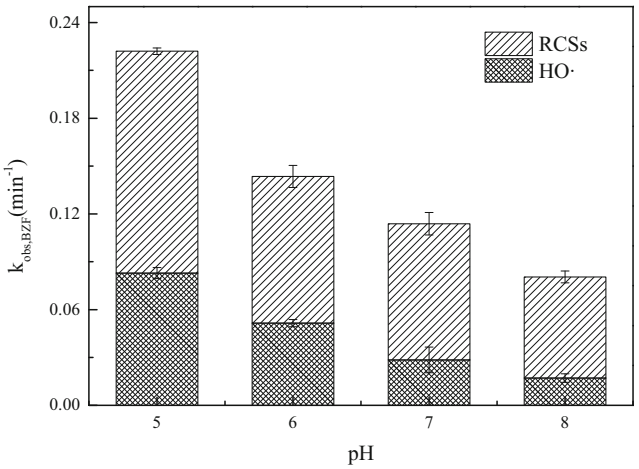

Fig. 7 Contributions of HO• and RCSs to BZF degradation in UV/chlorine process at different pH. Experimental conditions: $I_0 = 1.291 \times 10^{-7}$ Einstein L^{-1} s^{-1}, [NaClO] = 0.8 mM, [BZF] = 10 μM, [NB] = 10 μM, pH = 5.0 ~ 8.0, 10 mM phosphate buffer, $T = 20 \pm 1$ °C

Degradation pathways of BZF in UV/chorine process

Through LC-MS/MS analysis, 13 major intermediates were identified and they are shown in Table S2 in supporting information. Figure 8 showed the time-dependent evolution profiles of major degradation products of BZF in UV/chlorine process at pH 7.0. The pathways of BZF degradation in UV/chlorine process are proposed based on the identified products, as given in Fig. 9. As shown, four sites of BZF were proposed to be reactive (Fig. 9), and could be attacked by the radical (HO• and RCSs) in UV/chlorine process (Xu et al. 2016). Five newly detected chlorine-containing intermediates were obtained (as marked with solid brackets) compared with the traditional HO• based AOPs, such as UV/H_2O_2, UV/TiO_2, and catalytic ozonation process (Lambropoulou et al. 2008;

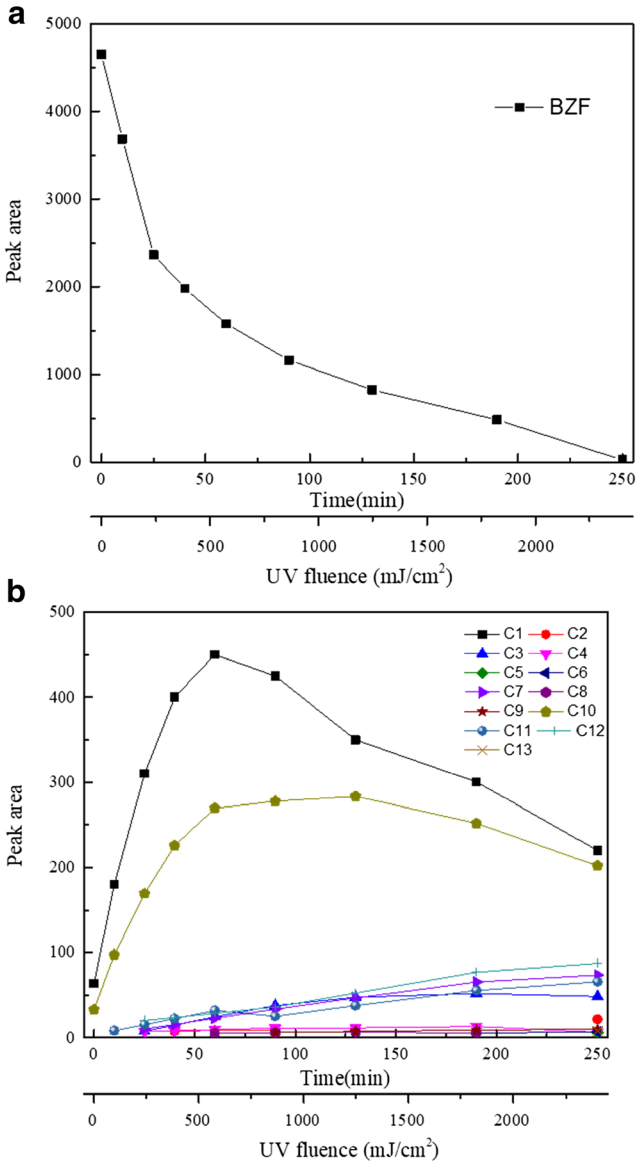

Fig. 8 Changes of degradation products during the reaction time in UV/chlorine process

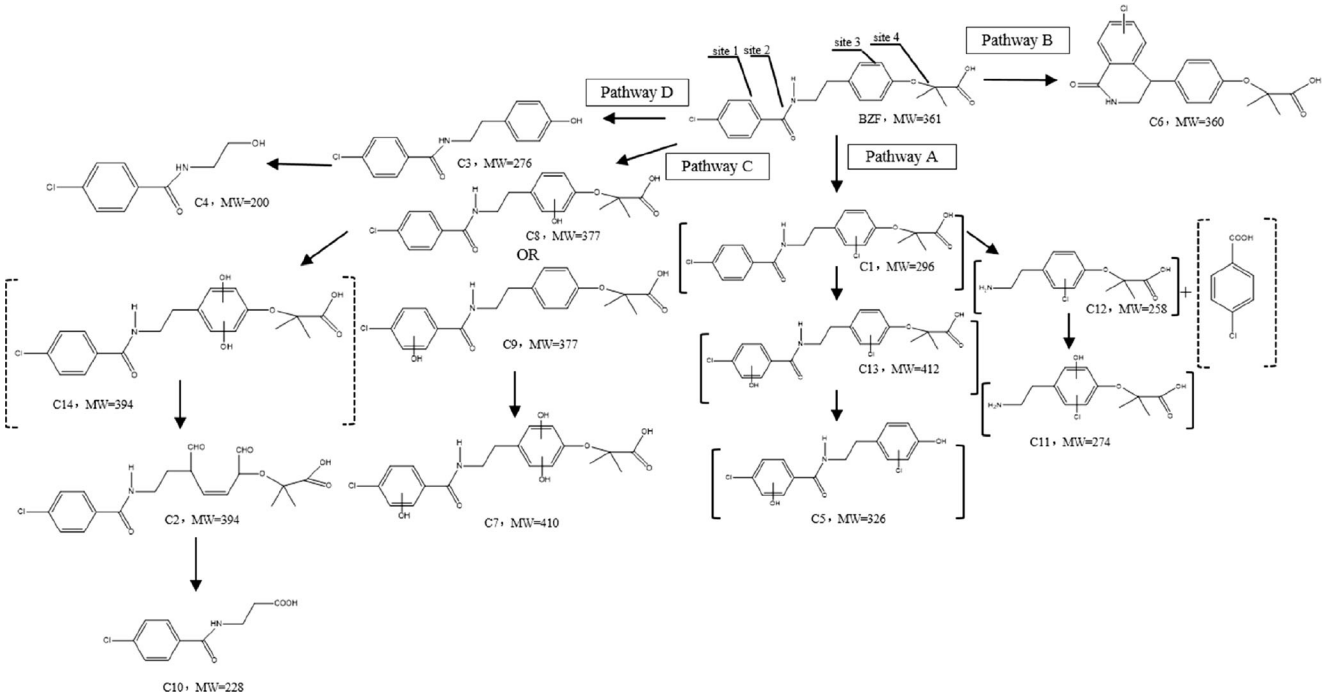

Fig. 9 BZF degradation pathways in UV/chlorine process

Xu et al. 2016; Yuan et al. 2012). The products with dotted line were suspected according to degradation pathway. Initially, the degradation products C1 and C10 increased rapidly during BZF degradation in UV/chlorine process, reached their peak values within 75 min and decreased then. Other products (C2 ~ C9, C11 ~ C13) increased continuously in the whole reaction time. Two reaction processes (pathway A and C) were suggested to be the main pathways based on the peak area of the intermediates.

Chlorine substitution and hydroxylation intermediates were observed during BZF degradation, as shown in pathway A. The monochloro compound C1 was formed, which could be ascribed to the oxidation of BZF by RCSs. The reactive Cl• added into site 3 in BZF, yielding a carbon-centered radical (as shown in Fig. S4 in supporting information), followed by oxygen addition and subsequently elimination of the perhydroxyl radicals (HOO•), leading to the chlorine substitution intermediate C1 (Wu et al. 2016). In order to enhance the formation of BZF degradation intermediates for detection, higher concentration of BZF (i.e., 0.5 mM) was applied. This suggested that BZF could efficiently compete with $HClO/ClO^-$ for the Cl• radicals consumption, thus resulted in the increasing contribution of Cl• to BZF degradation, and the subsequent production of C1 from Cl• additional reaction. It was reported that the chlorine preferred to substitute hydrogen in the benzene ring rather than in the aliphatic structure (Xiang et al. 2016). Due to the electron-withdrawing effect of chlorine, the chlorine ring has lower reactivity than the phenoxy ring (Martino et al. 1999). Therefore, chlorine substitution occurred in phenoxy ring which was also proved by product C1. Subsequently, HO• is susceptible to attacking chlorine ring (Gonçalves et al. 2012), which results in the formation of hydroxylated products (including compounds C13, C11) via the oxidation of C1 and C12. Furthermore, C5 and C12 were formed by HO• and/or RCSs attacking sites 4 and 2, respectively. Compared with the hydroxylated degradation route as discussed following (often happened in the HO•-basedAOPs), this chlorine substitution route (pathway A) is unique in UV/chlorine process (Wang et al. 2012).

A variety of hydroxylated intermediates were detected by LC-MS/MS, with the hydroxylation on the benzene ring occurring in a stepwise manner. This was similar with that in the typical HO•-based AOPs, such as catalytic ozonation process (Li et al. 2014). The monohydroxylated intermediates identified during this study were characterized as C8 (attacking on the phenoxy ring) and C9 (attacking on the chlorine-containing ring). In this step, the hydroxylation was formed in the ortho and meta orientation in either the chlorine or the phenoxy ring. The further oxidation on the monohydroxylated benzene ring could result in the formation of polyhydroxylated intermediates, such as C7 and C14 (Dantas et al. 2007). The continuous oxidation of C14 could lead to the cleavage of the aryloxy-carbon bond on the phenoxy ring (C2), resulting in the opening of this ring (C10). This route was denoted as pathway C. Besides, C3 and C4 were formed via the oxidation of sites 3 and 4 in BZF, which was denoted as pathway D.

In the pathway B, the m/z of product C6 was 359 while the parent compound m/z was 361. The appearance of this compound implied that the structure has a double bond or cyclization within the molecule (Razavi et al. 2009). It should be noted that the formation of a double bond was unreasonable, and the alternative mechanism that accounted for the compound C6 was shown in Fig. S5. This possible explanation is described briefly as that HO• attacked at the aromatic ring (addition of -OH), followed by cyclization with loss of HOH.

Conclusion

The UV/chlorine process could effectively degrade BZF, which followed the pseudo-first-order kinetics, and the observed rate constant in UV/chlorine process was 3.4 times and 1.9 times higher than that in the UV/H_2O_2 and UV/$S_2O_8^{2-}$ process, respectively. With the increase of chlorine dosage from 0.1 to 1.0 mM, the continuously increased $k_{obs,BZF}$ could be attributed to the increasing contribution of ClO•, which was verified by the Matlab modeling results. The BZF degradation was enhanced with the increase of Cl^- (0 ~ 200 mM), inhibited with the increase of HA (0 ~ 5.0 mg L^{-1}), and nearly not influenced by HCO_3^- (0 ~ 40 mM). $k_{obs,BZF}$ decreased while the contribution of RCSs increased as pH increased from 5.0 to 8.0. The degradation pathway of BZF included hydroxylation and chlorine substitution, and sustained through further oxidation to generate acylamino cleavage and demethylation products.

The chlorine-containing intermediates were detected in LC-MS/MS which indicated that disinfection byproducts and more attention should be paid for the toxicity assessment in further studies.

Funding information This work was supported by the National Natural Science Foundation of China (51578066 and 51608036), the Beijing Natural Science Foundation (No. 8152022), and the Fundamental Research Funds for the Central Universities (No. 2015ZCQ-HJ-02).

References

Beretta M, Britto V, Tavares TM, da Silva SMT, Pletsch AL (2014) Occurrence of pharmaceutical and personal care products (PPCPs) in marine sediments in the Todos os Santos Bay and the north coast of Salvador, Bahia, Brazil. J Soils Sediments 14:1278–1286

Buxton GV, Greenstock CL, Helman WP, Ross AB (1988) Critical review of rate constants for reactions of hydrated electrons, hydrogen atoms and hydroxyl radicals (·OH/·O⁻) in aqueous solution. J Phys Chem Ref Data 17:513–886

Cai M-Q, Feng L, Jiang J, Qi F, Zhang L-Q (2013) Reaction kinetics and transformation of antipyrine chlorination with free chlorine. Water Res 47:2830–2842

Carranzo IV (2012) APHA, AWWA, WEF. "standard methods for examination of water and wastewater." Anales de Hidrología Médica 5

Cermola M, DellaGreca M, Iesce M, Previtera L, Rubino M, Temussi F, Brigante M (2005) Phototransformation of fibrate drugs in aqueous media. Environ Chem Lett 3:43–47

Dantas RF, Canterino M, Marotta R, Sans C, Esplugas S, Andreozzi R (2007) Bezafibrate removal by means of ozonation: primary intermediates, kinetics, and toxicity assessment. Water Res 41:2525–2532

Fang J, Fu Y, Shang C (2014) The roles of reactive species in micropollutant degradation in the UV/free chlorine system. Environ Sci-Wat Res 48:1859–1868

Gibs J, Stackelberg PE, Furlong ET, Meyer M, Zaugg SD, Lippincott RL (2007) Persistence of pharmaceuticals and other organic compounds in chlorinated drinking water as a function of time. Sci Total Environ 373:240–249

Glassmeyer S, Shoemaker J (2005) Effects of chlorination on the persistence of pharmaceuticals in the environment. Bull Environ Contam Toxicol 74:24–31

Gonçalves A, Órfão JJ, Pereira MFR (2013) Ozonation of bezafibrate promoted by carbon materials. Appl Catal B Environ 140:82–91

Gonçalves AG, JJ Ó, Pereira MF (2012) Catalytic ozonation of sulphamethoxazole in the presence of carbon materials: catalytic performance and reaction pathways. J Hazard Mater 239-240:167–174

Guan YH, Ma J, Li XC, Fang JY, Chen LW (2011) Influence of pH on the formation of sulfate and hydroxyl radicals in the UV/peroxymonosulfate system. Environ Sci-Wat Res 45:9308

Guo Z-B, Lin Y-L, Xu B, Huang H, Zhang T-Y, Tian F-X, Gao N-Y (2016) Degradation of chlortoluron during UV irradiation and UV/chlorine processes and formation of disinfection by-products in sequential chlorination. Chem Eng J 283:412–419

Hessler DP, Gorenflo V, Frimmel FH (2010) Degradation of aqueous atrazine and metazachlor solutions by UV and UV/H_2O_2—influence of pH and herbicide concentration Abbau von Atrazin und metazachlor in wäßriger Lösung durch UV und UV/H2O2—Einfluß von pH und Herbizid-Konzentration. CLEAN Soil Air Water 21:209–214

Huerta-Fontela M, Galceran MT, Ventura F (2011) Occurrence and removal of pharmaceuticals and hormones through drinking water treatment. Water Res 45:1432–1442

Kim I, Tanaka H (2009) Photodegradation characteristics of PPCPs in water with UV treatment. Environ Int 35:793–802

Kim I, Yamashita N, Tanaka H (2009) Photodegradation of pharmaceuticals and personal care products during UV and UV/H_2O_2 treatments. Chemosphere 77:518–525

Kim SD, Cho J, Kim IS, Vanderford BJ, Snyder SA (2007) Occurrence and removal of pharmaceuticals and endocrine disruptors in South Korean surface, drinking, and waste waters. Water Res 41:1013–1021

Kong X, Jiang J, Ma J, Yang Y, Liu W, Liu Y (2016) Degradation of atrazine by UV/chlorine: efficiency, influencing factors, and products. Water Res 90:15–23

Kosma CI, Lambropoulou DA, Albanis TA (2010) Occurrence and removal of PPCPs in municipal and hospital wastewaters in Greece. J Hazard Mater 179:804–817

Lambropoulou D, Hernando M, Konstantinou I, Thurman E, Ferrer I, Albanis T, Fernández-Alba A (2008) Identification of photocatalytic degradation products of bezafibrate in TiO 2 aqueous suspensions by liquid and gas chromatography. J Chromatogr A 1183:38–48

Lee W, Westerhoff P, Yang X, Shang C (2007) Comparison of colorimetric and membrane introduction mass spectrometry techniques for chloramine analysis. Water Res 41:3097–3102

Lee Y, von Gunten U (2010) Oxidative transformation of micropollutants during municipal wastewater treatment: comparison of kinetic aspects of selective (chlorine, chlorine dioxide, ferrate VI, and ozone) and non-selective oxidants (hydroxyl radical). Water Res 44:555–566

Li H, Xu B, Qi F, Sun D, Chen Z (2014) Degradation of bezafibrate in wastewater by catalytic ozonation with cobalt doped red mud:

efficiency, intermediates and toxicity. Appl Catal B Environ 152–153:342–351

Lyon BA, Milsk RY, Deangelo AB, Simmons JE, Moyer MP, Weinberg HS (2014) Integrated chemical and toxicological investigation of UV-chlorine/chloramine drinking water treatment. Environ Sci-Wat Res 48:6743–6753

Mártire DO, Rosso JA, Bertolotti S, Le Roux GC, Braun AM, Gonzalez MC (2001) Kinetic study of the reactions of chlorine atoms and $Cl_2^{\bullet-}$ radical anions in aqueous solutions. II. Toluene, benzoic acid, and chlorobenzene. J Phys Chem A 105:5385–5392

Martino M, Rosal R, Sastre H, Díez FV (1999) Hydrodechlorination of dichloromethane, trichloroethane, trichloroethylene and tetrachloroethylene over a sulfided Ni/Mo–γ-alumina catalyst. Appl Catal B Environ 20:301–307

Mitch WA, Sedlak DL (2004) Characterization and fate of N-nitrosodimethylamine precursors in municipal wastewater treatment plants. Environ Sci-Wat Res 38:1445–1454

Mompelat S, Le Bot B, Thomas O (2009) Occurrence and fate of pharmaceutical products and by-products, from resource to drinking water. Environ Int 35:803–814. https://doi.org/10.1016/j.envint.2008.10.008

Rahn RO, Stefan MI, Bolton JR, Goren E, Shaw PS, Lykke KR (2003) Quantum yield of the iodide-iodate chemical actinometer: dependence on wavelength and concentrations. Photochem Photobiol 78:146–152

Razavi B, Song W, Cooper WJ, Greaves J, Jeong J (2009) Free-radical-induced oxidative and reductive degradation of fibrate pharmaceuticals: kinetic studies and degradation mechanisms. J Phys Chem A 113:1287–1294

Simazaki D, Fujiwara J, Manabe S, Matsuda M, Asami M, Kunikane S (2008) Removal of selected pharmaceuticals by chlorination, coagulation–sedimentation and powdered activated carbon treatment. Water Sci Technol 58:1129–1135

Szabó RK (2010) Decomposition of some pharmaceuticals by advanced oxidation processes University of Szeged Doctoral School of Environmental Sciences

Trovó AG, Melo SAS, Nogueira RFP (2008) Photodegradation of the pharmaceuticals amoxicillin, bezafibrate and paracetamol by the photo-Fenton process—application to sewage treatment plant effluent. J Photochem Photobiol A Chem 198:215–220

Wang D, Bolton JR, Hofmann R (2012) Medium pressure UV combined with chlorine advanced oxidation for trichloroethylene destruction in a model water. Water Res 46:4677–4686

Wang WL, Wu QY, Huang N, Wang T, Hu HY (2016) Synergistic effect between UV and chlorine (UV/chlorine) on the degradation of carbamazepine: influence factors and radical species. Water Res 98:190–198

Watkinson A, Murby E, Kolpin D, Costanzo S (2009) The occurrence of antibiotics in an urban watershed: from wastewater to drinking water. Sci Total Environ 407:2711–2723

Watts MJ, Linden KG (2007) Chlorine photolysis and subsequent OH radical production during UV treatment of chlorinated water. Water Res 41:2871–2878

Wols BA, Harmsen DJH, Beerendonk EF, Hofman-Caris CHM (2015) Predicting pharmaceutical degradation by UV (MP)/H_2O_2 processes: a kinetic model. Chem Eng J 263:336–345

Wu Y, Bianco A, Brigante M, Dong W, Sainteclaire PD, Hanna K, Mailhot G (2015) Sulfate radical photogeneration using Fe-EDDS: influence of critical parameters and naturally occurring scavengers. Environ Sci-Wat Res 49:14343

Wu Z, Fang J, Xiang Y, Shang C, Li X, Meng F, Yang X (2016) Roles of reactive chlorine species in trimethoprim degradation in the UV/chlorine process: kinetics and transformation pathways. Water Res 104:272–282

Xiang Y, Fang J, Shang C (2016) Kinetics and pathways of ibuprofen degradation by the UV/chlorine advanced oxidation process. Water Res 90:301

Xu B, Qi F, Sun D, Chen Z, Robert D (2016) Cerium doped red mud catalytic ozonation for bezafibrate degradation in wastewater: efficiency, intermediates, and toxicity. Chemosphere 146:22–31

Yang X et al (2016) PPCP degradation by UV/chlorine treatment and its impact on DBP formation potential in real waters. Water Res 98:309–318

Yuan H, Zhang Y, Zhou X (2012) Degradation of bezafibrate with UV/H_2O_2 in surface water and wastewater treatment plant effluent. CLEAN Soil Air Water 40:239–245

Z S, C L, M B, JR B, MG E (2014) Application of a solar UV/chlorine advanced oxidation process to oil sands process-affected water remediation. Environ Sci-Wat Res 48:9692–9701

Zhang X, Li W, Rd BE, Wang X, Ren P (2015) UV/chlorine process for ammonia removal and disinfection by-product reduction: comparison with chlorination. Water Res 68:804–811

Zhao X, Chen Z-L, Wang X-C, Shen J-M, Xu H (2014) PPCPs removal by aerobic granular sludge membrane bioreactor. Appl Microbiol Biotechnol 98:9843–9848